1   **Auxin is not asymmetrically distributed in initiating Arabidopsis leaves**

2   **Neha Bhatia[1] and Marcus G. Heisler[1*]**

3

4   **Affiliations**

5   [1]School of Life and Environmental Sciences, University of Sydney, NSW, Australia

6   *Author for correspondence: Marcus G Heisler (marcus.heisler@sydney.edu.au)

7   **Abstract**

8   It has been proposed that asymmetric auxin levels within initiating leaves help

9   establish leaf polarity, based in part on observations of the DII auxin sensor. Here we

10   show that the mDII control sensor also exhibits an asymmetry and that according to

11   the ratio-metric auxin sensor R2D2, no obvious asymmetry in auxin exists. Together

12   with other recent findings, our results argue against the importance of auxin

13   asymmetry in establishing leaf polarity.

14

15   **Results and Discussion**

16   The leaves of seed plants are usually flat with distinct cell types making up

17   their dorsal (upper) and ventral (lower) tissues. A fundamental question in plant

18   development is how this dorsal-ventral polarity is first specified. Studies based on

19   wounding experiments have suggested the presence of an inductive signal originating

20   from the meristem that promotes dorsal identity in the adaxial (adjacent to the

21   meristem) tissues of the leaf primordium[1,2]. However more recently, it was found that

22   exogenous application of the plant hormone auxin to tomato leaf primordia resulted in

23   the formation of radialized leaves that appeared ventrilized. Hence, relatively high

24   levels of auxin are proposed to promote ventral or inhibit dorsal leaf cell fate[3].

25   Extending these conclusions, it was also proposed that an asymmetry in the auxin

26   distribution across the leaf adaxial-abaxial axis at leaf initiation acts to help specify

27   leaf polarity during regular development[3]. A critical piece of evidence supporting this

28   latter proposal is that an auxin sensor, the DII[4,5] indicates low levels of auxin in

29   adaxial leaf tissues compared to abaxial tissues at leaf initiation[3]. Hence asymmetries

30   in auxin concentrations between the adaxial and abaxial leaf tissues, as a result of

31   PIN1 mediated auxin transport, are proposed to help establish leaf polarity[3]. Building

32   on this conclusion, a more recent study proposed that low levels of auxin in adaxial

33 tissues are necessary to restrict the expression of the WOX1 and PRS genes to the
34 middle domain, since auxin promotes their expression[6]. Finally, the reported
35 asymmetry in auxin has also been linked to asymmetries in the mechanical properties
36 of leaf tissues and their morphogenesis[7].
37
38 Despite these studies, reason to reassess the role of any asymmetry in auxin in
39 specifying leaf polarity has arisen due to the recent finding that the expression
40 patterns of genes involved in leaf dorsoventrality are already patterned in meristem
41 tissues where leaves originate, with little change occurring to their expression during
42 organ initiation. Hence leaf polarity appears pre-patterned [8]. Furthermore, rather than
43 compromise dorsal cell fate, auxin was found to promote dorsal cell fate by
44 maintaining Class III HD-ZIP expression and repressing KAN1 expression in the
45 adaxial cells of organ primordia[8], which is the opposite of what would be expected
46 according to the auxin asymmetry hypothesis. In addition, Caggiano et al. (2017) also
47 found that exogenous auxin application to young leaf primordia did not influence the
48 spatial pattern of WOX1 and PRS, only the intensity of expression[8]. This also
49 conflicts with the proposal that low levels of auxin are required in adaxial leaf tissues
50 to prevent ectopic WOX1 and PRS expression as previously proposed[6].
51
52 Given the concerns listed above, we decided to examine the distribution of auxin
53 during leaf initiation using not only by the DII sensor assessed in previous studies but
54 also, by looking more closely at the expression pattern of the non-auxin degradable
55 mDII auxin sensor control[4] as well as the ratiometric R2D2 auxin sensor[9]. We
56 initially focused on the first two leaves three and four days after stratification (DAS),
57 when these leaves are initiating as well as a day later as they begin to elongate and
58 included the PIN1-GFP marker in our analysis to correlate auxin levels with PIN1
59 expression and polarity. At 3DAS, the expression patterns of REV and KAN1 are
60 already polar within such primordia, although the FIL expression domain at this stage
61 of development is still being refined[8]. Also at this stage, PIN1 is polarized towards the
62 distal tip of leaf primordia but has reversed polarity away from the primordia, towards
63 the meristem, in cells adjacent to the primordia on the adaxial side. According to the
64 ratio-metric auxin sensor R2D2, auxin concentrations were relatively low in adaxial
65 cells of the primordia but also low in abaxial and lateral regions proximally (Fig1-a
66 and d; Fig.S1). High levels of auxin were only found in more distal regions towards

2

67 the tip of the primordia, matching the overall pattern of signal from PIN1-GFP. No
68 obvious asymmetry in signal between the adaxial and abaxial sides of the primordia
69 was observed. This same overall pattern of signal was found in 16 out of 18 leaves
70 that were examined. At 4DAS, the auxin distribution according to the R2D2 sensor
71 was more uniform although higher levels of auxin appeared associated with the
72 vasculature, again correlating with PIN1 expression (n=12/12 leaves) (Fig. 1 g and j).
73
74 As our results using the R2D2 auxin sensor indicate a different auxin distribution
75 compared to that reported previously using the DII marker [3], we next re-examined the
76 pattern of DII auxin sensor expression at the same developmental stages. In contrast
77 to the R2D2 pattern, the DII pattern showed an asymmetry of expression in leaf
78 primordia at 3 DAS, indicating relatively low auxin levels in adaxial primordium
79 cells, as found previously. DII signal appeared strongest in the adaxial epidermis but
80 was also stronger in the adaxial sub-epidermal cell layer compared to abaxial
81 epidermal and sub-epidermal cell layers (Fig.1- b, e, h and Fig. S2) (n=18/18 leaves).
82 One day later, although DII signal was still higher in the adaxial cells of the
83 primordia, it started to show a relatively increased expression in the abaxial sub-
84 epidermal layers as well compared to earlier stage (n=13/14 leaves) (Fig1-k). Overall
85 our results using the DII marker are similar to those obtained previously and
86 consistent with the proposal that there are low levels of auxin in the adaxial regions of
87 leaf primordia, in contrast to our results using the R2D2 sensor. Given this
88 discrepancy, we next examined the expression of the mDII sensor which is driven by
89 the same 35S promoter as the DII sensor but is not auxin sensitive. Surprisingly we
90 found that, like the DII results, expression of the mDII marker was also higher in the
91 adaxial cells of the primordia (n= 16/16 leaves) (Fig.1-c,f,i and Fig.S3). The pattern
92 appeared almost identical to the pattern found using the DII marker except that the
93 mDII marker also showed high levels of expression in the shoot meristem whereas the
94 DII sensor did not (compare Fig1-b,c; Fig S2 a-h and Fig S3 a-f). The similarity of
95 expression between DII and mDII was also apparent at 4DAS when the leaves had
96 started to elongate (Fig.1-l) (n=14/14 leaves). To verify the auxin sensitivity of the
97 sensors used we imaged seedlings before and after treatment with 5mM NAA and
98 found a strong decrease in DII expression compared to mDII and an increase in the
99 ratio of VENUS compared to tdTomato signal for the R2D2 sensor, consistent with an
100 increase in auxin levels (Figure S4).

101

102　All together these results indicate that the asymmetry in expression found previously

103　for the DII auxin sensor in very young leaf primordia[3] is not due to an asymmetry in

104　auxin levels but rather, likely due to differences in transcription driven by the 35S

105　promoter used to drive both DII and mDII in adaxial compared to abaxial leaf tissues.

106　We note that although a single section showing control expression of mDII in older

107　leaves was cited by Guan et al., (2017)[10], our results show that this information was

108　not adequate for assessing similarities and differences between DII and mDII at early

109　developmental stages. To check whether adaxial expression in leaf primordia is a

110　characteristic common to other reporters driven by the 35S promoter, we also

111　examined the expression of 35S::H2B-mRFP1 and 35S::EGFP-LTI6b which had

112　previously been combined into the same plant line by crossing[11]. Surprisingly the

113　expression patterns for these markers were not only different to the mDII marker but

114　also different to each other with the H2B marker showing stronger expression in the

115　adaxial and abaxial epidermis and the LTI6b marker showing a more uniform pattern

116　(Fig. S5). These results reveal that even when the same promoter is utilized to drive

117　FP (fluorescent protein) expression, distinct differences in intensity patterns can occur

118　*in planta*. This may be due to differences in the position of T-DNA insertion in the

119　genome or differences in the surrounding DNA of the vector used. All together then,

120　our results highlight the importance of using ratio-metric sensors for *in vivo*

121　measurements since otherwise it is difficult to adequately control for differences in

122　signal intensity due to promoter activity or other confounding factors. Finally, while

123　the R2D2 marker utilizes a single transgene to express two distinct FPs from two

124　identical promoters[9], a potentially improved approach to assess auxin levels *in vivo*

125　may be to utilize a single promoter to drive the auxin-dependent degradation domain

126　II from Aux/IAA proteins linked to a tandem fusion of fast and slowly folding FP

127　variants, such as VENUS and mCherry. Such an approach can enable a more direct

128　readout of protein degradation rates[12,13] and therefore potentially improve

129　measurements of relative auxin concentration.

130

131　While our findings are inconsistent with the proposal that asymmetries in the auxin

132　distribution influence leaf polarity[3], pattern WOX/PRS gene expression [6] or regulate

133　tissue mechanics[7], they also leave other observations unexplained. In particular, to

134　understand the apparent ventrilization of leaf primordia in tomato in response to

135 exogenous auxin[3] will require further work in assessing how auxin distribution

136 patterns change in response to exogenous treatments and how auxin is distributed

137 during regular development in tomato, preferentially using a ratio-metric auxin sensor

138 such as R2D2.

139

140 **Methods**

141 **Plant material and growth conditions.**

142 Seeds of the plants expressing *p35S::DII-VENUS* and *p35S::mDII-VENUS*

143 transgenes (*Columbia* ecotype) were obtained from Dr. Teva Vernoux [4]. An

144 independent batch of seeds expressing *p35S::mDII-VENUS* transgenes (*Columbia*

145 ecotype) was also obtained from NASC (Arabidopsis stock center, NASC ID:

146 N799174) for analysis. R2D2 reporter line carrying *pPIN1::PIN1GFP* transgene

147 (*Landsberg* ecotype) has been described previously[9,14]. Seeds were germinated and

148 grown on GM medium (pH-7 with 1M KOH) containing 1% sucrose, 1X Murashige

149 and Skoog salts (Sigma M5524), MES 2-(MN-morpholino)- ethane sulfonic acid

150 (Sigma M2933), 0.8 % Bacto Agar (Difco), 1% MS vitamins (Sigma M3900) in long

151 day conditions.

152

153 **Confocal imaging and data analysis**

154 Seedlings aged 3DAS (days after stratification) and 4DAS were dissected as

155 described previously[14]. Dissected seedlings were then oriented appropriately to obtain

156 a view of the young leaves either from above or from the side. Seedlings were imaged

157 live, on a Leica TCS-SP5 upright confocal laser scanning microscope with hybrid

158 detectors (HyDs) using a 25X water objective (N.A 0.95). VENUS was imaged using

159 argon laser (excitation wavelength 514nm) while tdTomato was imaged using a white

160 light laser (excitation wavelength 561 nm). Z-stacks were acquired in a 512x512 pixel

161 format with section spacing of 1μm and line averaging 2.

162

163 Ratio-metric calculations for R2D2 auxin sensor were performed using ImageJ (FIJI,

164 https://fiji.sc) as described previously[14]. All the images were processed using IMARIS

165 9.0.0 (bit-plane). Optical sections (transverse or longitudinal) were reconstructed

166 using orthogonal slicer in IMARIS.

167

168

Auxin treatment

Seedlings aged 3DAS were dissected imaged and treated with approximately 10μL of 5mM NAA (1-Napthaleneacetic acid) solution in water (0.5M stock in 1M KOH) for 60 minutes and imaged again with same settings as prior to treatment.

173

180

References

1   Sussex, I. M. Morphogenesis in Solanum tuberosum I: experimental investigation of leaf dorsiventrality and orientation in the juvenile shoot. *Phytomorphology* **5**, 286-300 (1955).

2   Reinhardt, D., Frenz, M., Mandel, T. & Kuhlemeier, C. Microsurgical and laser ablation analysis of leaf positioning and dorsoventral patterning in tomato. *Development* **132**, 15-26 (2005).

3   Qi, J. *et al.* Auxin depletion from leaf primordia contributes to organ patterning. *Proc Natl Acad Sci U S A* **111**, 18769-18774, doi:10.1073/pnas.1421878112 (2014).

4   Brunoud, G. *et al.* A novel sensor to map auxin response and distribution at high spatio-temporal resolution. *Nature* **482**, 103-106, doi:10.1038/nature10791 (2012).

5   Vernoux, T. *et al.* The auxin signalling network translates dynamic input into robust patterning at the shoot apex. *Mol Syst Biol* **7**, 508, doi:10.1038/msb.2011.39 (2011).

6   Guan, C. *et al.* Spatial Auxin Signaling Controls Leaf Flattening in Arabidopsis. *Curr Biol* **27**, 2940-2950 e2944, doi:10.1016/j.cub.2017.08.042 (2017).

7   Qi, J. *et al.* Mechanical regulation of organ asymmetry in leaves. *Nat Plants* **3**, 724-733, doi:10.1038/s41477-017-0008-6 (2017).

8   Caggiano, M. P. *et al.* Cell type boundaries organize plant development. *eLife* **6**, doi:10.7554/eLife.27421 (2017).

9   Liao, C. Y. *et al.* Reporters for sensitive and quantitative measurement of auxin response. *Nat Methods* **12**, 207-210, 202 p following 210, doi:10.1038/nmeth.3279 (2015).

10   Wang, Y. *et al.* The Stem Cell Niche in Leaf Axils Is Established by Auxin and Cytokinin in Arabidopsis. *Plant Cell* **26**, 2055-2067, doi:10.1105/tpc.114.123083 (2014).

210   11   Federici, F., Dupuy, L., Laplaze, L., Heisler, M. & Haseloff, J. Integrated
211   genetic and computation methods for in planta cytometry. *Nature*
212   *Methods* **9**, 483-U104, doi:10.1038/nmeth.1940 (2012).
213   12   Khmelinskii, A. *et al.* Tandem fluorescent protein timers for in vivo
214   analysis of protein dynamics. *Nat Biotechnol* **30**, 708-714,
215   doi:10.1038/nbt.2281 (2012).
216   13   Barry, J. D., Dona, E., Gilmour, D. & Huber, W. TimerQuant: a modelling
217   approach to tandem fluorescent timer design and data interpretation for
218   measuring protein turnover in embryos. *Development* **143**, 174-179,
219   doi:10.1242/dev.125971 (2016).
220   14   Bhatia, N. *et al.* Auxin Acts through MONOPTEROS to Regulate Plant Cell
221   Polarity and Pattern Phyllotaxis. *Curr Biol* **26**, 3202-3208,
222   doi:10.1016/j.cub.2016.09.044 (2016).

223

224

225

226

227

228
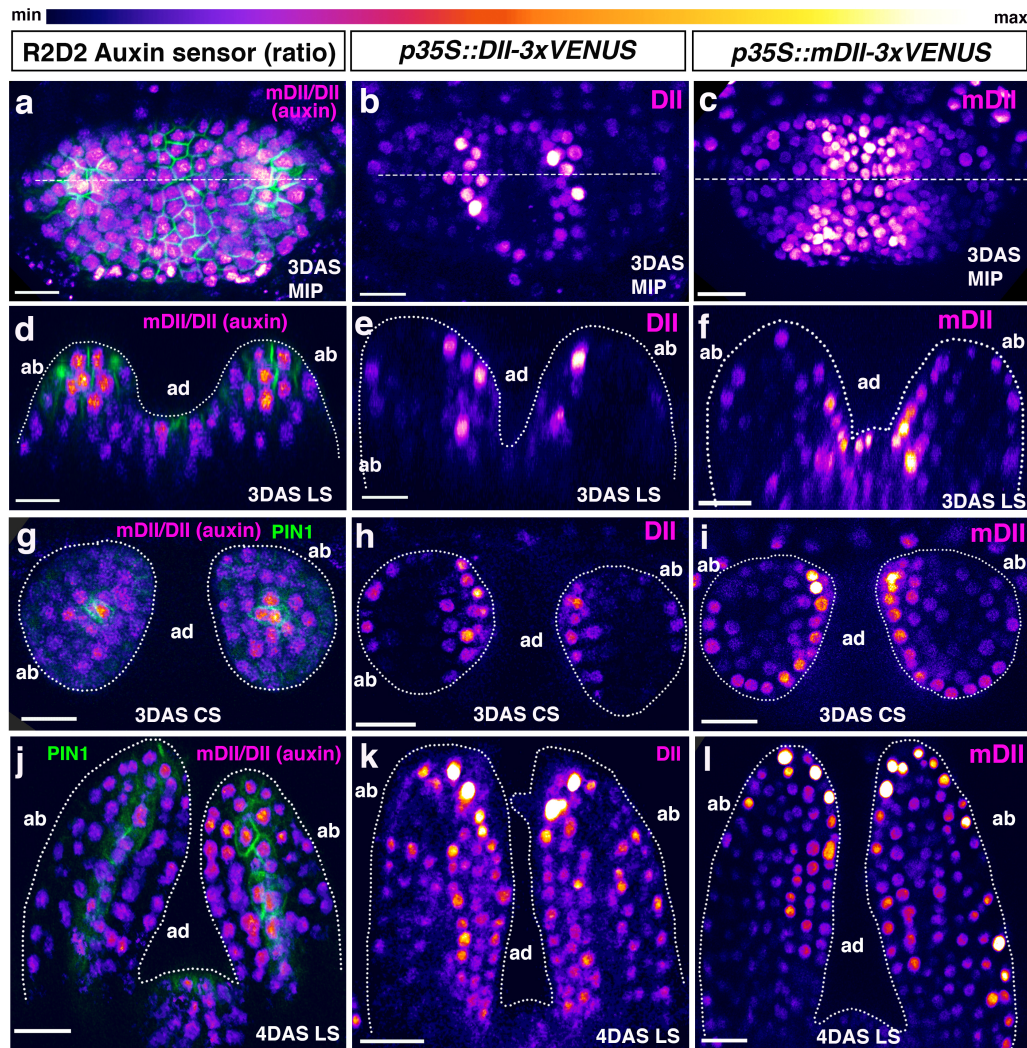
Figure 1 Predicted auxin distribution in young leaves as indicated by different auxin sensors.

(a-c) Confocal projections of *Arabidopsis* seedlings aged 3DAS (days after stratification) showing predicted auxin distribution based on the ratio-metric auxin sensor R2D2 (magenta) along with PIN1-GFP (green) (a); expression pattern of *p35S::DII-VENUS* (magenta) (b) and *p35S::mutatedDII-VENUS* (mDII, magenta) (c). (d-f) Longitudinal reconstructed optical sections of (a-c), respectively, along the dashed lines. (g-i) Representative examples of transverse reconstructed optical sections of 3DAS Arabidopsis seedlings showing predicted auxin distribution as indicated by the R2D2 sensor along with PIN1-GFP expression (g), DII-VENUS expression (h) and mDII-VENUS expression (i). R2D2 auxin sensor indicates low but symmetric auxin levels on adaxial and abaxial sides and relatively high auxin levels at the distal tip and in the provasculature where PIN1 expression is also high (d, g). DII-

8

242   VENUS is more strongly expressed adaxially indicating low auxin levels on the

243   adaxial side of the leaves relative to the abaxial side. However, mDII-VENUS also

244   shows high expression on the adaxial side of the leaf (compare e, h with f, i) and in

245   the shoot meristem. **(j-l)** Representative examples of longitudinal reconstructed

246   optical sections of 4DAS Arabidopsis seedlings showing predicted auxin distribution

247   by R2D2 sensor along with PIN1-GFP expression (green) (i), DII-VENUS expression

248   (j) and mDII-VENUS expression (k). At this stage, the R2D2 sensor indicates a more

249   uniform auxin distribution in the leaf but higher auxin levels in the vasculature where

250   PIN1-GFP expression is also high (j). DII-VENUS shows slightly high expression in

251   adaxial cells and an absence of expression in the vasculature (k). mDII-VENUS

252   shows a similar pattern to DII but is also expressed in the vasculature (l). Scale bars

253   15μm (a-i) and 20μm (j-l).

254

9
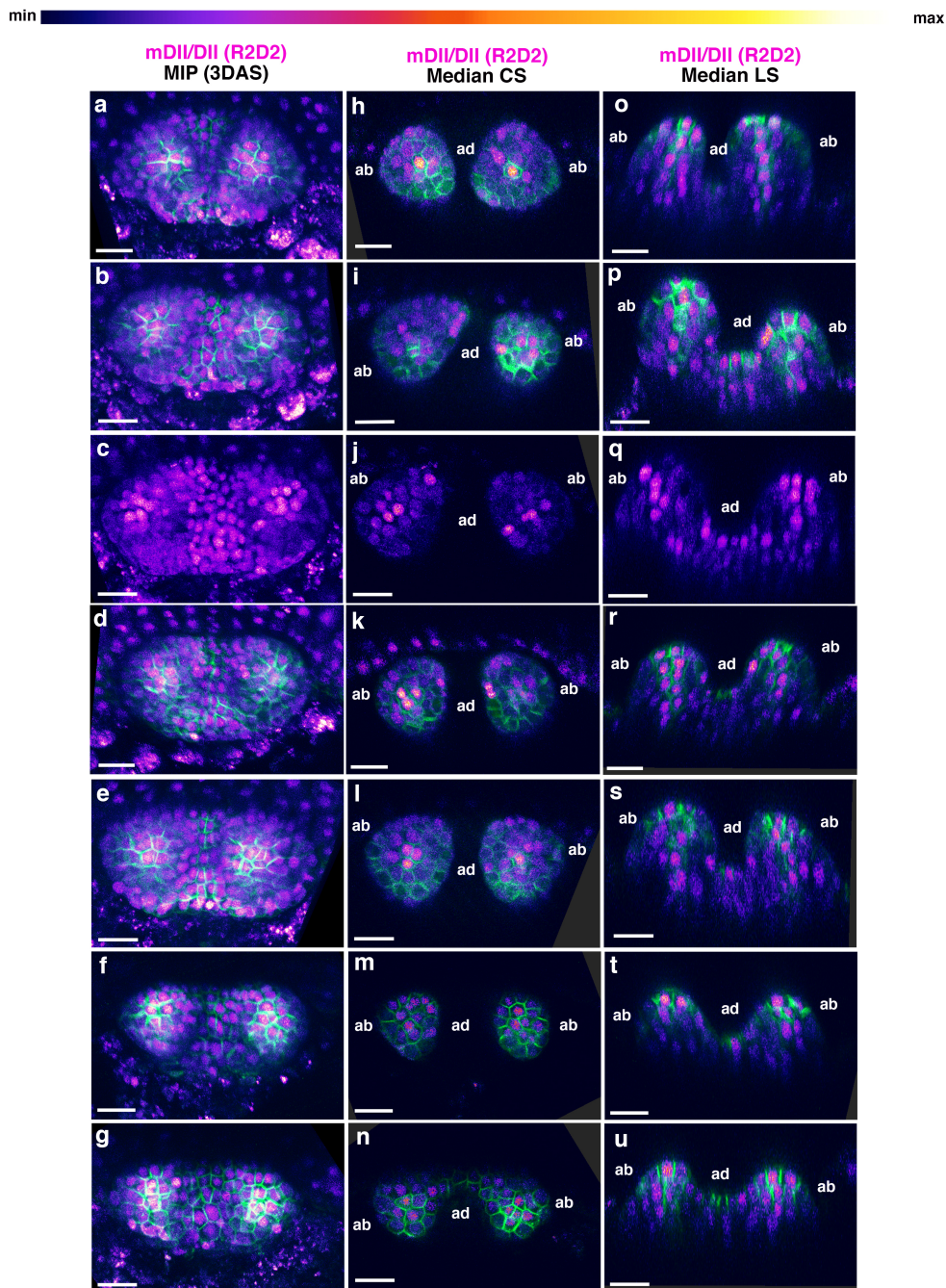
255   FigureS1

256

257   **FigureS1 Additional examples of R2D2, ratio-based predictions of auxin**

258   **distribution in 3DAS old Arabidopsis seedlings. (a-g)** Confocal projections of

259   *Arabidopsis* seedlings aged 3DAS (days after stratification) showing predicted auxin

260   distribution based on the ratio-metric auxin sensor R2D2 (magenta) along with PIN1-

261   GFP (green). **(h-n)** Median transverse optical sections of (a-g). **(o-u)** Median

262   longitudinal optical sections of (a-g). Scale bars 20μm (a-u).
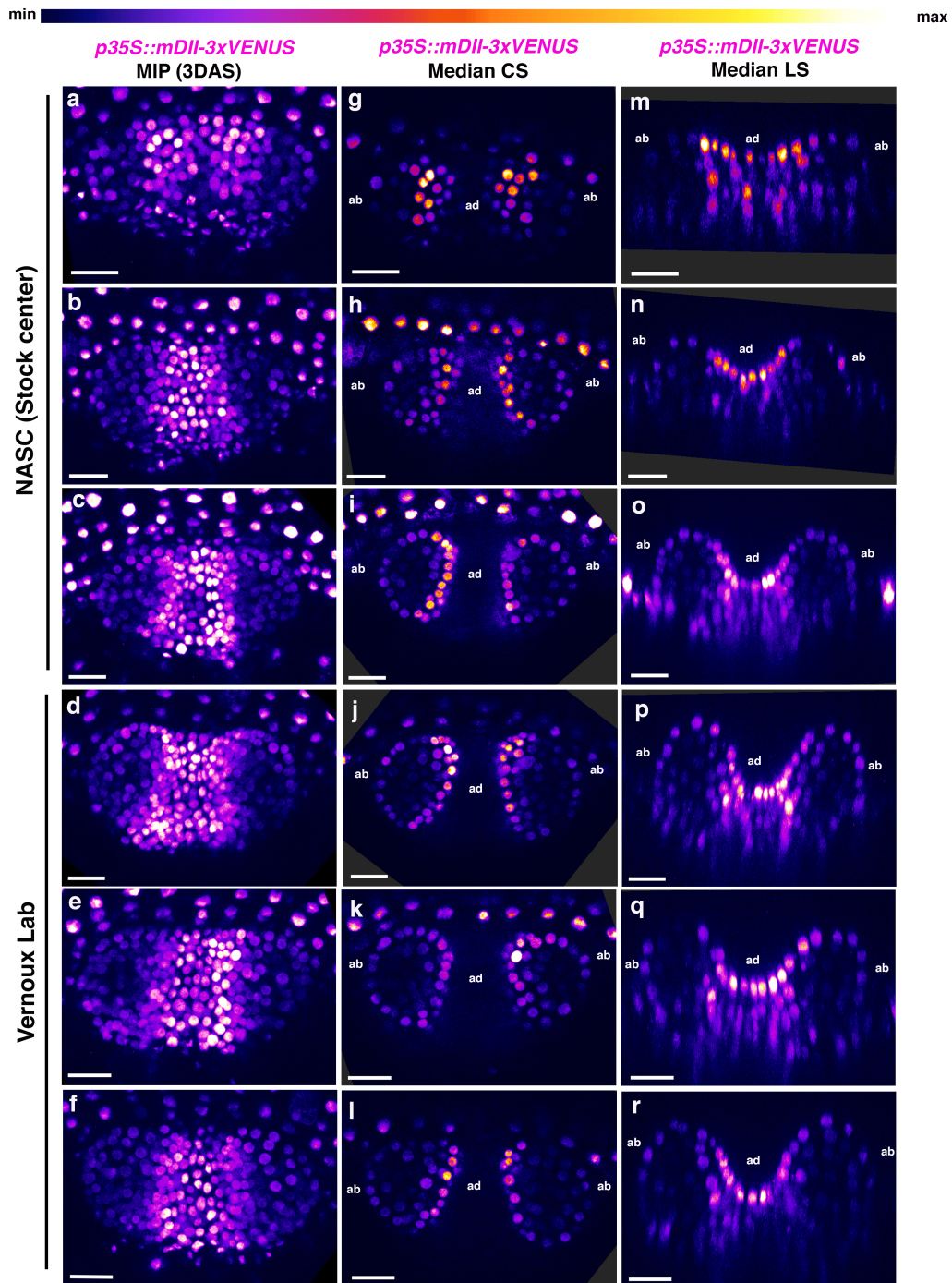
263

264

265   Figure S2

266
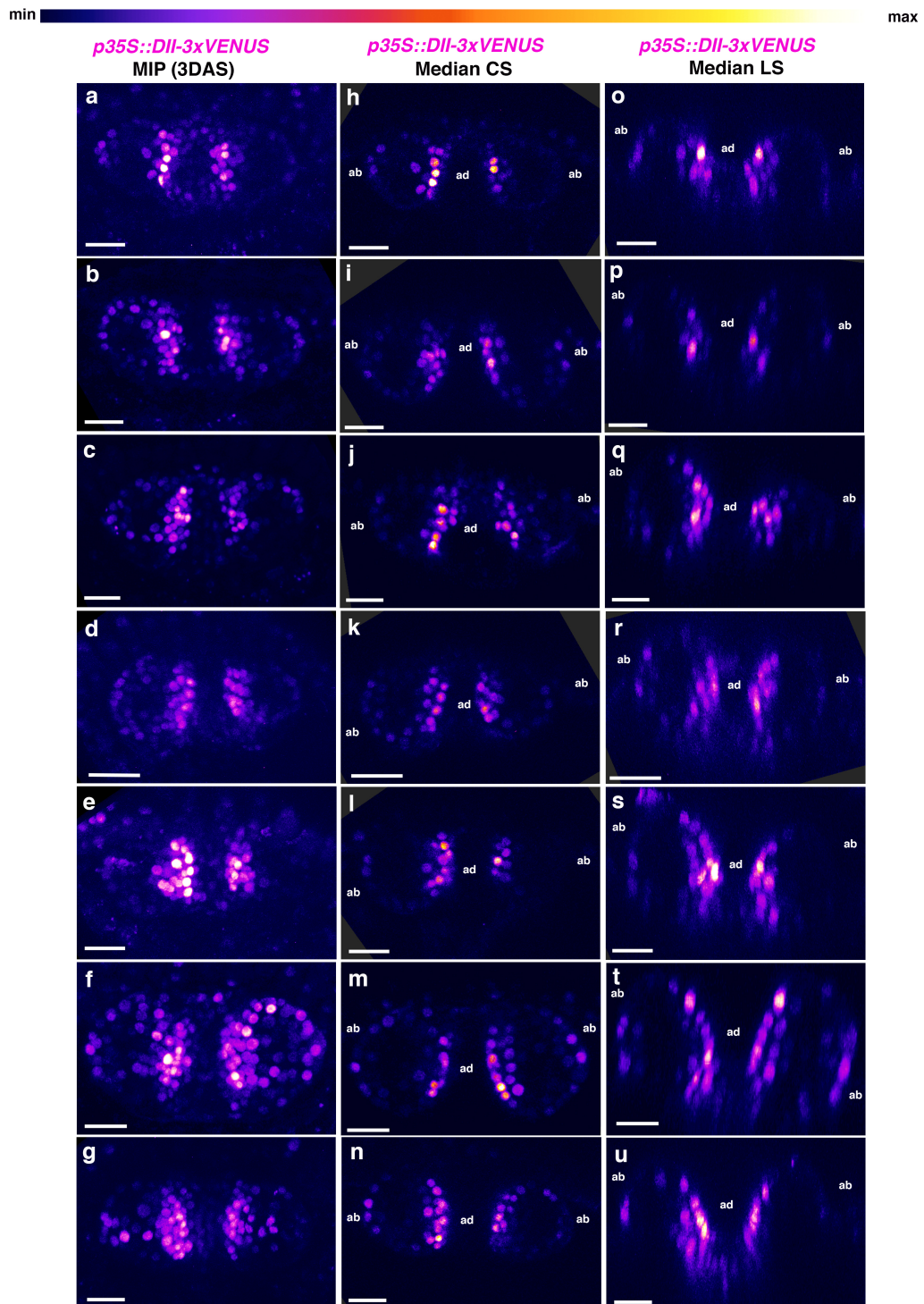
FigureS1 Additional examples *p35S::DII-3xVENUS-N7* expression in 3DAS old Arabidopsis seedlings. (a-g) Confocal projections of *Arabidopsis* seedlings aged 3DAS (days after stratification) showing expression pattern of p35s::DII-3xVENUS-

270   N7 sensor (magenta). **(h-n)** Median transverse optical sections of (a-g). **(o-u)** Median

271   longitudinal optical sections of (a-g). Scale bars 20μm (a-u).

272   FigureS3

273

274   **FigureS1 Additional examples of *p35S::mDII-3xVENUS-N7* expression in 3DAS**

275   **old Arabidopsis seedlings. (a-f)** Confocal projections of *Arabidopsis* seedlings aged

276   3DAS (days after stratification) showing expression pattern of p35s::mDII-

277   3xVENUS-N7 sensor (magenta). Note that plants obtained from two different sources

13

278   showed similar expression pattern. **(h-l)** Median transverse optical sections of (a-f).

279   **(o-r)** Median longitudinal optical sections of (a-g). Scale bars 20μm (a-r).

280

281

282

283

284

285

286

287

288

289

290

291

292

293

294

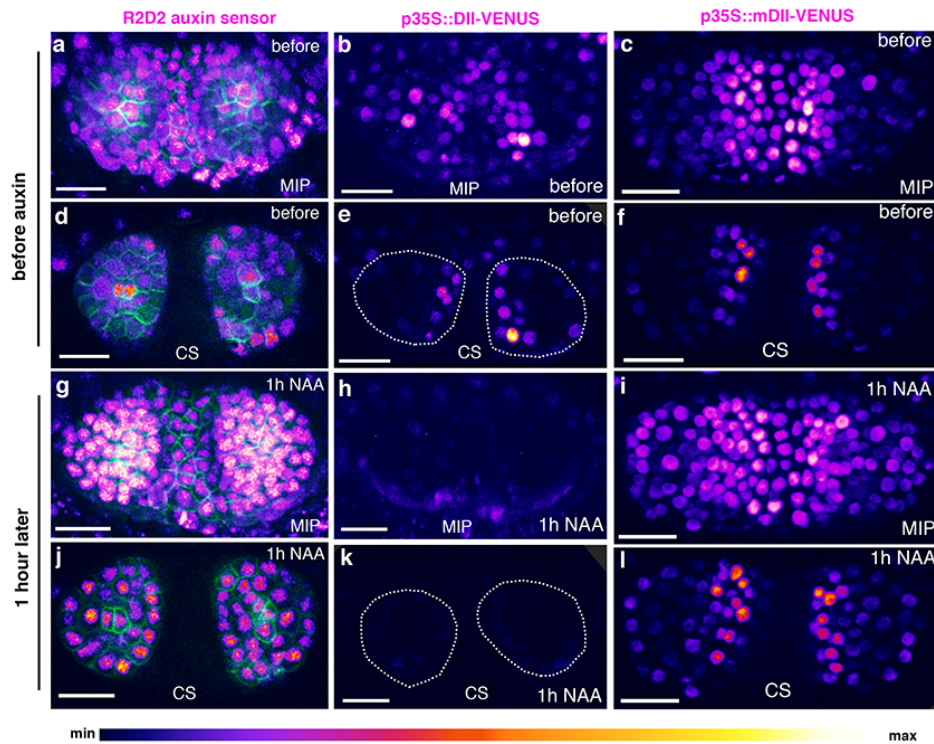295

296

297

298

299

300

301

302

303

304

305

306

307

308

309

310

311   FigureS4

312

**Figure S4 Response of different auxin sensors to external auxin application**

314

(a-f) Confocal projections (a-c) and transverse optical reconstructions (d-f) of *Arabidopsis* seedlings, 3DAS, showing predicted auxin distribution based on R2D2 ratio-metric sensor (magenta) along with PIN1-GFP expression in green (a,d), DII-VENUS sensor (magenta) (b,e) and mDII-VENUS sensor (magenta) (c, f) before auxin application. **(g-l)** Confocal projections (g-i) and transverse optical reconstructions (j-l) of *Arabidopsis* seedlings, 3DAS, showing predicted auxin distribution based on R2D2 ratio-metric sensor (magenta) along with PIN1-GFP expression in green (a,d), DII-VENUS sensor (magenta) (b,e) and mDII-VENUS sensor (magenta) (c, f) 1hour after the application of 5mM NAA. Note, R2D2 sensor indicates an increased and broadening of auxin levels after NAA application (compare d and j) (n=3/3). Consistently, DII-VENUS shows an attenuated expression within 1 hour of auxin application (compare b,e with h,j) (n=4/4). mDII-VENUS levels do not decrease upon auxin application (compare c,f with i,l) (n=4/4). Scale bars 20μm (a-l).

328

15

329   Figure S5

330

331

332
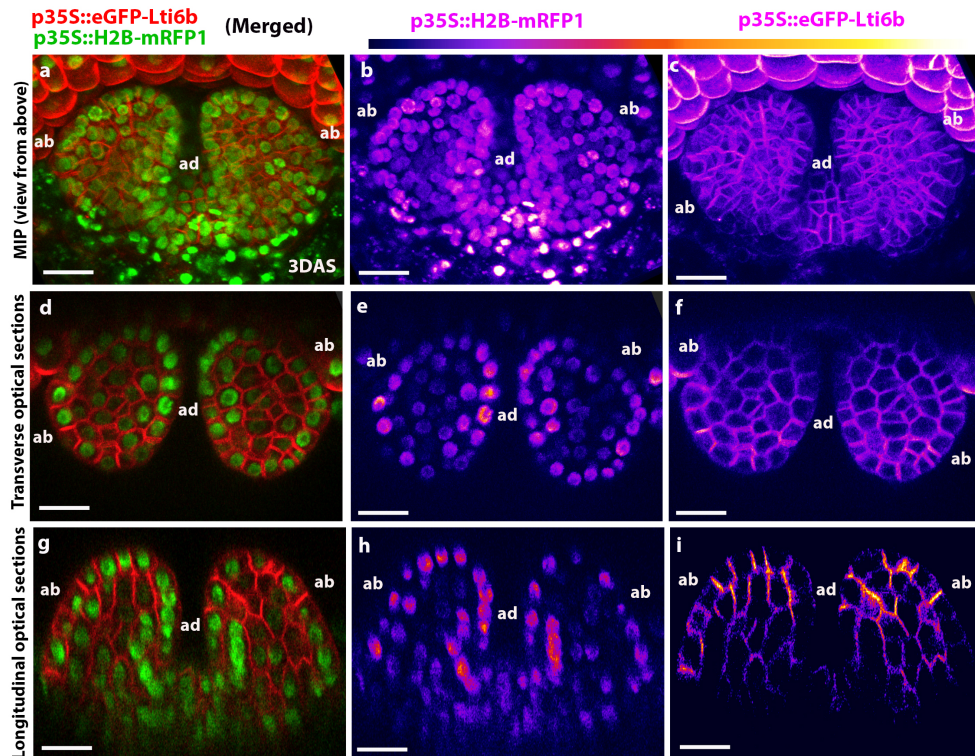
Figure S5 Different 35S promoter-driven reporter genes show different expression patterns in young leaves.

335

(a-c) Confocal projections of *Arabidopsis* seedlings aged 3DAS showing expression patterns of a *p35S:eGFP-Lti6b* (membrane marker, green) and *p35S::H2B-mRFP1*(nuclear marker red) together (a), *p35S::H2B-mRFP1* only (magenta) (b) and *p35S:eGFP-Lti6b* only (magenta) (c). **(d-f)** Transverse optical reconstructions of (a-c) respectively; merged (d), *p35S::H2B-mRFP1* only (magenta) (e) and *p35S:eGFP-Lti6b* only (magenta) (f). **(g-i)** Longitudinal optical reconstruction of (a-c) respectively; merged (g), *p35S::H2B-mRFP1* only (magenta) (h) and *p35S:eGFP-Lti6b* only (magenta) (i). Note *p35S::H2B-mRFP1* shows similarly high levels of expression in both adaxial (ad) as well as abaxial (ab) epidermal cell layers and weaker expression in the middle regions (e and h). However, *p35S:eGFP-Lti6b* shows no consistent asymmetry in expression throughout the leaf (f and i). Scale bars 20μm (a-i), (n=10 leaves).

348

16